Toward Waveform Nonlinear Optics Using Multimillijoule Sub-Cycle Waveform Synthesizers

Oliver D. Mücke, Shaobo Fang, Giovanni Cirmi, Giulio Maria Rossi, Shih-Hsuan Chia, Hong Ye, Yudong Yang, Roland Mainz, Cristian Manzoni, Paolo Farinello, Giulio Cerullo, and Franz X. Kärtner

(Invited Paper)

***Abstract*—Waveform nonlinear optics aims to study and control the nonlinear interactions of matter with extremely short optical waveforms custom-tailored within a single cycle of light. Different technological routes to generate such multimillijoule sub-optical-cycle waveforms are currently pursued, opening up unprecedented opportunities in attoscience and strong-field physics. Here, we discuss the experimental schemes, introduce the technological challenges, and present our experimental results on high-energy sub-cycle optical waveform synthesis based on (1) parametric amplification and (2) induced-phase modulation in a two-color-driven gas-filled hollow-core fiber compressor. More specifically, for (1), we demonstrate a carrier-envelope-phase (CEP)-stable, multimillijoule three-channel parametric waveform synthesizer generating a $>$2-octave-wide spectrum (0.52–2.4 μm). After two amplification stages, the combined 125-μJ output supports 1.9-fs FWHM waveforms; energy scaling to $>$2 mJ is achieved after three amplification stages. FROG pulse characterization of all three second-stage outputs demonstrates the feasibility to recompress all three channels simultaneously close to the Fourier limit and shows the flexibility of our intricate dispersion management scheme for different experimental situations. For (2), we generate CEP-stable 1.7-mJ waveforms covering 365–930 nm (measured at 1% of the peak intensity) obtained from induced-phase modulation in a two-color-driven gas-filled hollow-core fiber. Using custom-designed double-chirped mirrors and a UV spatial light modulator will permit compression close to the 0.9-fs FWHM transform limit. These novel sources will become versatile tools for controlling strong-field interactions in matter and for attosecond pump–probe spectroscopy using VIS/IR and XUV/soft-X-ray pulses.**

***Index Terms*—Ultrabroadband sources, parametric oscillators and amplifiers, gas-filled hollow-core fiber pulse compression, pulse synthesis, waveform nonlinear optics.**

I. Introduction and Motivation

THE generation of CEP-controlled light transients with durations below a single cycle of light is currently one of the most intriguing frontiers of ultrafast optics. This research field has attracted enormous attention from the ultrafast community not only because it overcomes the technological barrier imposed by the light period, but also because it opens the door to a previously inaccessible regime of extreme light-matter interactions. Recent technological advances enable control over the temporal profile of the electric field of a light pulse comparable to the one achievable, albeit at much lower frequencies, using electronic waveform generators, leading to a new research field known as *optical waveform electronics*. The capability to generate optical waveforms having an electric field profile $E(t)$ (and associated magnetic field) custom-tailored *within* an optical cycle of light in turn opens up a completely new regime of light-matter interactions, known as *waveform nonlinear optics* [1]–[4]. In this regime, the time-evolution of the electric field deviates strongly from a sinusoidal carrier-wave oscillation within a single cycle of light, so that the usual approximations of nonlinear optics break down, and new phenomena and opportunities arise. In high-harmonic generation (HHG) and attoscience, sub-cycle driving pulses will enable the efficient generation of intense isolated attosecond pulses (IAPs) [5], [6]. HHG in gases is an extreme nonlinear optical interaction, in which the electric field of the light pulse is high enough to lower the Coulomb potential of the atom or molecule and to extract an electron by tunnel ionization. The electron set free into the continuum is subsequently accelerated in the laser field and brought to recollide with the parent ion, leading to the emission of an XUV continuum by recombination into the ground state. The sequence of emission/recollision events during a driving pulse leads to the development of the harmonic structure of the HHG spectrum,

Manuscript received January 23, 2015; revised April 16, 2015; accepted April 21, 2015. This work was supported by the Center for Free-Electron Laser Science at DESY, the excellence cluster "The Hamburg Centre for Ultrafast Imaging—Structure, Dynamics and Control of Matter at the Atomic Scale" of the Deutsche Forschungsgemeinschaft, the ERC-Synergy grant AXSIS under Grant 609920, and by JRA-INREX from LASERLAB-EUROPE under Grant 284464, ECS Seventh Framework Programme. The work of C. Manzoni was supported by MIUR FIRB under Grant RBFR12SW0J. The work of G. Cerullo was supported by the European Research Council Advanced Grant STRATUS ERC-2011-AdG under Grant 291198. O. D. Mücke, S. Fang, and G. Cirmi contributed equally to this work. Corresponding authors: (e-mail: shaobo.fang@desy.de, giovanni.cirmi@cfel.de, oliver.muecke@cfel.de).

O. D. Mücke, S. Fang, G. Cirmi, G. M. Rossi, S.-H. Chia, H. Ye, Y. Yang, and R. Mainz are with the Ultrafast Optics and X-Rays Group, Center for Free-Electron Laser Science, Deutsches Elektronen-Synchrotron, 22607 Hamburg, Germany, and also with the Hamburg Center for Ultrafast Imaging, 22761 Hamburg, Germany (e-mail: oliver.muecke@cfel.de; shaobo.fang@desy.de; giovanni.cirmi@cfel.de; giulio.maria.rossi@cfel.de; shih-hsuan.chia@cfel.de; hong.ye@cfel.de; yudong.yang@cfel.de; roland.mainz@cfel.de).

C. Manzoni and G. Cerullo are with the IFN-CNR, Dipartimento di Fisica, Politecnico di Milano, I-20133 Milan, Italy, and also with the Istituto di Fotonica e Nanotecnologie, Consiglio Nazionale delle Ricerche, 00185 Rome, Italy (e-mail: cristian.manzoni@polimi.it; giulio.cerullo@fisi.polimi.it).

P. Farinello is with the Laser Source Laboratory, Dipartimento di Ingegneria Industriale e dell'Informazione, Università di Pavia, I-27100 Pavia, Italy (e-mail: paolo.farinello01@universitadipavia.it).

F. X. Kärtner is with the Ultrafast Optics and X-Rays Group, Center for Free-Electron Laser Science, Deutsches Elektronen-Synchrotron, 22607 Hamburg, Germany, with the Hamburg Center for Ultrafast Imaging, 22761 Hamburg, Germany, with the Physics Department, University of Hamburg, 22761 Hamburg, Germany, and also with the Department of Electrical Engineering and Computer Science and Research Laboratory of Electronics, Massachusetts Institute of Technology, Cambridge, MA 02139, USA (e-mail: franz.kaertner@desy.de).

Color versions of one or more of the figures in this paper are available online at http://ieeexplore.ieee.org.

Digital Object Identifier 10.1109/JSTQE.2015.2426653

1077-260X © 2015 IEEE. Personal use is permitted, but republication/redistribution requires IEEE permission.
See http://www.ieee.org/publications_standards/publications/rights/index.html for more information.

which corresponds to a train of XUV pulses. Generation of an IAP requires isolation of a single recollision event, which is traditionally performed in different ways: either by spectrally filtering the high-energy cutoff portion of the XUV emission [4] or by using different gating techniques [polarization gating, ionization gating, (generalized) double optical gating, etc.] to suppress all but a single recollision process [7]. These approaches typically significantly reduce the energy of the IAP. The use of a sub-cycle optical waveform as a driving pulse for HHG would enable to naturally limit emission/recollision to a single event, greatly increasing the efficiency of IAP generation, as already demonstrated in first experiments [5], [6]. Additionally, a sub-cycle optical waveform would permit control of the tunnel ionization step [8] and enable to precisely manipulate the electron trajectory in the continuum, optimizing its kinetic energy and the corresponding energy cutoff of the HHG spectrum, realizing experimentally the theoretically predicted "perfect waveform" for HHG [9]–[14].

If suitably scaled in energy [15], sub-cycle waveforms will enable to extend waveform nonlinear optics to the relativistic interaction regime [16]. One important application is laser wakefield acceleration of electrons, which uses the longitudinal component of the driving field to increase the electron kinetic energy along the propagation direction, thus producing quasi-monoenergetic electron bunches over much shorter propagation distances with respect to standard radio-frequency accelerators [17]–[20]. Such electron pulses, with energy meanwhile reaching up to 4.2 GeV [21], can be used to drive tabletop ultrashort X-ray sources [22], [23] with exceptional brilliance and to probe photoinduced dynamics by ultrafast electron/X-ray diffraction.

The same sub-femtosecond control of the photoelectron trajectories, as achieved in the gas phase leading to HHG and IAP generation, can be extended to the solid state and in particular to electrons in metal nanostructures. Sharp metal nanotapers irradiated with CEP-controlled few-cycle optical waveforms generate coherent electron wave packets highly confined both in time and in space [24]–[26]. Sub-cycle optical waveforms would allow to steer, switch and control such wave packets, enabling radically new implementations of electron diffraction and electron microscopy [27] with unprecedented combination of spatial and temporal resolution. Sub-cycle optical waveforms also find applications in the study of strong-field light-matter interactions in solids [28]–[37] and for the control of electric currents in (and thereby emitted HHG from) semiconductors [38], [39] and insulators on the sub-cycle timescale. Such extreme interactions of short optical waveforms with solids are expected to enable the field of *lightwave nanoelectronics*, which is based on nanocircuits, which accept data as light in the form of plasmons. The highly nonlinear response of nanomaterials to strong laser fields will permit the switching of currents within such nanocircuits with frequencies approaching the petahertz domain. This will increase by several orders of magnitude the clock rate of electronic devices, which is currently limited to the multigigahertz range by fundamental bottlenecks in their architecture [33], [40], [41].

The generation of optical waveforms with sub-cycle control poses great technological and experimental challenges. The recent development of linear and nonlinear techniques allows the routine generation of few-optical-cycle pulses by different processes, such as emission from laser oscillators [42], nonlinear spectral broadening in a guiding medium [43], [44], filamentation in gases [45]–[48], or optical parametric amplification (OPA) [49], [50]. In order to break the few-optical-cycle limit and to shorten the pulse duration below a single optical cycle, the most promising strategy is coherent combination, or synthesis, of pulses with different colors generated from separate sources. As discussed in greater detail in [2], the key ingredients of coherent waveform synthesis are (i) the generation of an ultrabroad spectrum, (ii) extremely precise spectral phase control over the whole bandwidth, (iii) sub-cycle timing synchronization as well as tight stabilization of the relative phases between the different sub-pulses, and (iv) CEP stability required for generating reproducible electric-field transients. Depending on the requirements (energy, spectral bandwidth, pulse duration, repetition rate etc.) of the targeted application, different technological approaches have recently been pursued to generate such sub-cycle waveforms. Waveform synthesis starting from supercontinuum generation in gas-filled hollow-core fiber (HCF) compressors represents a rather mature technology and has permitted the generation of sub-cycle $\sim$300-μJ optical pulses (covering 260–1100 nm) [3], [51], [52]. However, the scalability of gas-phase broadening schemes in terms of pulse energy and repetition rate seems to be limited by ionization losses, detrimental nonlinearities, thermal-related problems and damage of materials. In contrast, parametric waveform synthesizers offer much better prospects for simultaneously scaling up both the pulse energy to the multimillijoule range and the repetition rate to tens or hundreds of kilohertz, which makes them very attractive for various applications in next-generation light sources such as SLAC, European XFEL, SACLA, FERMI and ELI-ALPS, targeting such extreme operation parameter ranges. Another very appealing feature of parametric amplification is the straightforward spectral extension into the mid-IR region for the realization of bright coherent tabletop HHG sources in the water-window and keV X-ray region [53], [54].

Waveform synthesizers can also be classified into (i) sequential and (ii) parallel schemes [2]. In sequential parametric waveform synthesizers [15], [55], different spectral regions are amplified in subsequent amplification stages employing different phase-matching conditions without ever splitting the beam. The sequential approach has the advantage of completely removing the need to synchronize the sub-pulses, which comes at the expense of the big challenge to compress the entire huge bandwidth with the same dispersive elements at once. In contrast, parallel synthesis schemes [56]–[58] offer much greater flexibility by splitting the bandwidth into separate channels, in which the different spectral regions can individually be amplified and/or compressed. Importantly, the coherent synthesis of reproducible waveforms in parallel schemes requires sub-cycle timing synchronization as well as tight stabilization of the relative phases between the different channels, and CEP stability. Some schemes, such as the recently demonstrated frequency-domain OPA (FOPA) [59] can even feature (positive and negative) aspects of both parallel and sequential synthesis schemes:

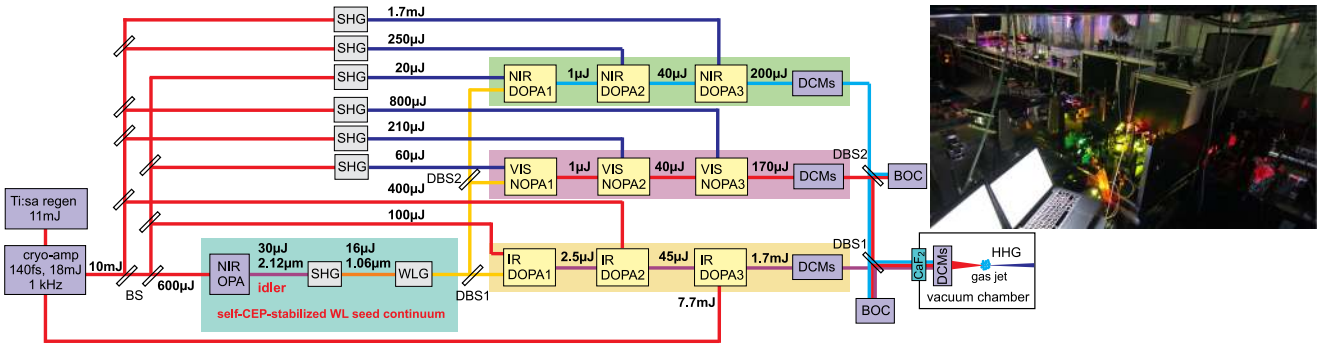

Fig. 1. (Left) Scheme of the >2-octave-wide multi-mJ parametric waveform synthesizer. BS, beam splitter; SHG, second-harmonic generation; WLG, white-light generation; DBS, dichroic beam splitter; NOPA, non-collinear OPA; DOPA, degenerate OPA; DCMs, double-chirped mirrors; BOC, balanced optical cross-correlator. (Right) Photo of the experiment, the BOC setup can be seen in the front.

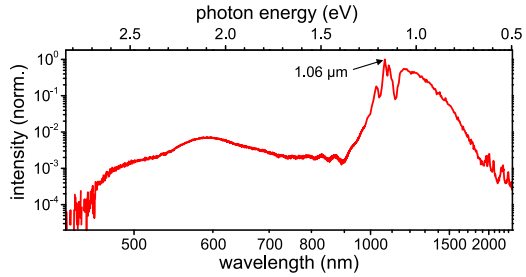

Fig. 2. Passively CEP-stabilized white-light seed continuum generated in a 3-mm-thick YAG crystal pumped by the second harmonic (1.06 μm) of the CEP-stable idler [63] of the NIR OPA as shown in Fig. 1.

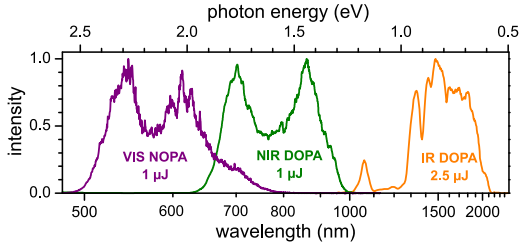

Fig. 3. Output spectra and energies from the first OPA stages.

the FOPA scheme is parallel with respect to the amplification process; it is sequential with respect to dispersion management, bandwidth limitations (e.g., due to the diffraction efficiency curve of the gratings), and the intrinsic stability of the relative timing and phase.

In our earlier works, we already demonstrated coherent pulse synthesis from the combination of ultrabroadband 870-nm and 2.15-μm pulses based on optical parametric chirped-pulse amplification (OPCPA) resulting in a 15-μJ sub-cycle waveform [56], [57] and also combining two optical parametric amplifiers (OPAs) with 1-2 μJ energy each [58]. Here, in Section II we present our ongoing development of a novel multimillijoule 3-channel parametric waveform synthesizer (shown in Fig. 1) for generating a >2-octave-wide spectrum with ~1.9-fs transform-limited (TL) duration. In Section III, we present our recent progress toward a waveform synthesizer based on a two-color-driven gas-filled hollow-core fiber (HCF) compressor (shown in Fig. 13), which is expected to be compressible close to the 0.9-fs FWHM TL.

II. Three-Channel Parametric Waveform Synthesizer

Starting point of the synthesizer [60]–[62] shown in Fig. 1 is a cryogenically cooled Ti:sapphire chirped-pulse amplifier (140 fs, 18 mJ, 0.8 μm, 1 kHz). We generate a CEP-stable supercontinuum (0.5–2.5 μm) shown in Fig. 2 by white-light generation in a 3-mm-thick YAG crystal pumped by the second harmonic (1.06 μm) of the self-CEP-stabilized idler [63] of a NIR OPA. The continuum is split with custom-designed dichroic beam splitters (DBSs) (which will also be used for the final beam recombination, see Section II-A) and seeds three OPA channels, a VIS non-collinear OPA (NOPA), a NIR and an IR degenerate OPA (DOPA) channel, pumped by the pulses at 0.8 μm (IR DOPA) and its second harmonic at 0.4 μm (VIS NOPA, NIR DOPA). All OPAs employ type-I BBO crystals (the phase-matching angle θ is 31°, 29°, and 20° for the VIS NOPA, NIR DOPA and IR DOPA, respectively). After parametric amplification, the three OPA channel outputs can individually be recompressed using custom-tailored double-chirped mirrors (DCMs), as discussed in Section II-A. Finally, in order to synthesize a coherent ultrashort waveform from these OPA channels, the relative timing of the pulses will be tightly locked using feedback loops with balanced optical cross-correlators (BOCs), that can achieve sub-cycle synchronization with <30-as rms timing jitter [56]–[58].

Figs. 3 and 4(a) show the measured output spectra from the first and second amplification stages operating in parallel, respectively. After the second stage, the VIS NOPA and NIR DOPA continuously cover the region from 520 to 960 nm, the IR DOPA spectrum extends from 1130 to 2290 nm. The TL pulse duration from the synthesis of these three spectra (assuming 1:1.3:1 intensity weighting and all CEPs to be 0) is 1.9 fs FWHM, corresponding to 0.7 optical cycles at 785 nm center wavelength, as shown in Fig. 4(b).

Afterwards, the energy can be scaled to the multimillijoule level in the third amplification stages (see Fig. 5). First, the energy of the IR DOPA is increased to 1.7 mJ in a third IR DOPA stage employing a 4-mm-thick BBO crystal pumped by 7.7 mJ pulses, i.e., we achieve a pump-signal conversion efficiency of 22%. Although a strong energy imbalance between the channels is obviously suboptimum for waveform synthesis,

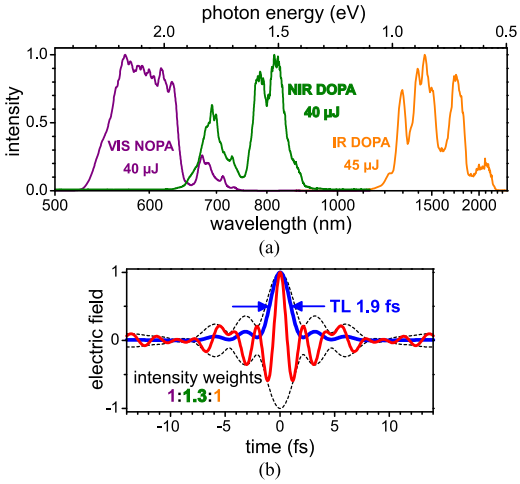

Fig. 4. (a) Output spectra and energies from the second OPA stages. (b) The TL pulse synthesized from the weighted spectra in (a) and assuming all CEPs to be 0 corresponds to a 1.9-fs FWHM pulse duration. The red curve is the electric field $E(t)$, the dashed curves indicate the field envelope $\tilde{E}(t)$, the intensity profile $I(t)$ is the blue trace.

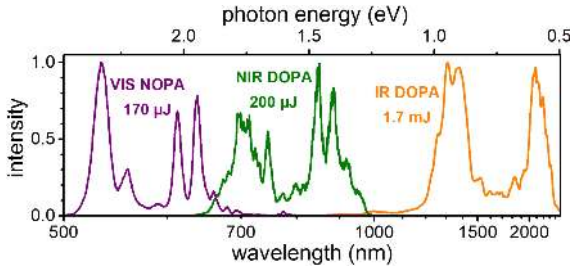

Fig. 5. Output spectra and energies from the third stages of the VIS NOPA/NIR DOPA/IR DOPA channels. These spectra support 5.6/5.2/5.2-fs pulses corresponding to 2.9/2.1/1.1 optical cycles at 573 nm/750 nm/1390 nm center wavelengths, respectively. Note that the bandwidths of the second stages were slightly increased compared to the spectra shown in Fig. 4(a), to optimize the seeding of the third stages.

we intentionally targeted a predominantly high energy of this IR DOPA channel, aiming to use it later for long-wavelength HHG into the water-window region and potentially even beyond [53], [54]. Second, depending on the requirements of the attoscience experiment that we want to perform in the future, we can split the remaining pump pulses for scaling the energy in VIS NOPA and NIR DOPA. Using 2-mm-thick BBOs, we so far have obtained the VIS NOPA3 and NIR DOPA3 spectra and energies shown in Fig. 5.

One comment on the slight modulations seen in the spectra shown in Figs. 3–5: All OPA stages are carefully designed and optimized, such that the peak pump intensity is always $\sim$50 GW/cm^2, i.e., safely below the BBO damage threshold, below the onset of self-phase modulation (SPM) of the pump, and (as discussed in Section II-A) optimized to suppress buildup of superfluorescence in the OPA chains. Therefore, these slight spectral modulations most likely originate from residual group-delay (GD) ripples of the dispersive mirrors in the parametric amplification.

To guarantee long-term and day-to-day reproducible operation, we employ three active beam-pointing stabilization units to

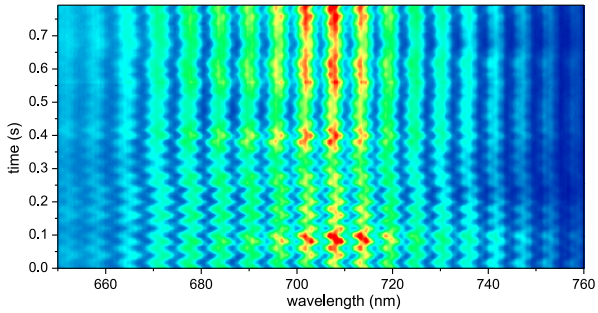

Fig. 6. Interference fringes observed in the region of spectral overlap between the VIS NOPA1 and NIR DOPA1 (*without* timing lock), confirming coherence between the two OPA outputs. The slow oscillatory behavior of the fringes, which is of environmental origin, can straightforwardly be eliminated by feedback control. The shown interferogram was acquired with 4 ms integration time, 4 ms additional waiting time.

fix (1) the input beam of the NIR OPA used for seed generation, (2) the beam, from which all pumps of the first and second stages are derived, and (3) the beam, from which all pumps of the third stages are derived. When the beam-pointing stabilizers are active, we typically observe residual beam-pointing fluctuations $<$1% of the beam diameter.

The feasibility of performing a coherent pulse synthesis from the different channels was confirmed by the observation of interference fringes in the region of spectral overlap, as shown in Fig. 6 for the VIS NOPA1 and NIR DOPA1.

A. Precise Dispersion Management Over More Than Two Octaves

One key enabling technology for generating multimillijoule $\sim$2-fs pulses and actually delivering them to an attoscience experiment is precise dispersion management over more than two octaves in optical bandwidth. The dispersion management, as sketched in the dispersion map shown in Fig. 7, is a multifaceted huge challenge, that needs to fulfill a number of requirements: (1) temporal optimization of ultrabroadband OPAs in *each* stage in terms of bandwidth and conversion efficiency, as well as for suppression of the buildup of superfluorescence in the amplification chain, (2) flexible (ideally programmable, of course) dispersion compensation that can be adapted to different experimental situations, including final compression of the high-energy waveform to a duration close to the Fourier limit, (3) avoidance/reduction of the B-integral due to intense pulse propagation in Kerr media (e.g., beam splitter substrates, entrance window of the vacuum chamber), that would destroy the pulse quality.

Ultrabroadband multi-stage high-gain parametric amplifiers require a very careful design to maximize both the conversion efficiency and bandwidth, while simultaneously suppressing superfluorescence [64]. In each amplification stage, the seed pulse duration must carefully be matched to the temporal window of high parametric gain defined by the pump pulse duration in order to prevent an undesirable buildup of detrimental superfluorescence background in the amplification chain. This becomes especially crucial for obtaining clean pulses from the final millijoule-level booster amplification stages. As investigated

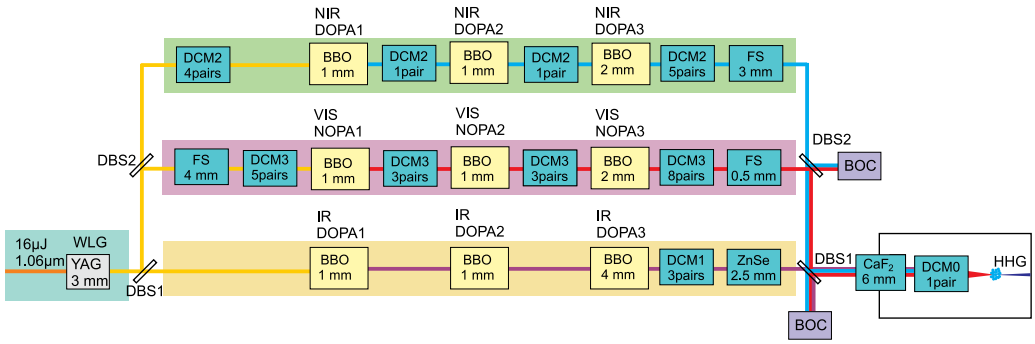

Fig. 7. Map of the dispersion management: WLG, white-light generation; DBS, dichroic beam splitter; FS, fused silica; DCM, double-chirped mirror (number of pairs as indicated).

in [64], a small compromise in amplifier bandwidth relative to the full phase-matching bandwidth, by use of the appropriate seed chirp, both maximizes the efficiency-bandwidth product and optimizes the signal-to-noise ratio. On the other hand, maximization of signal bandwidth was found to significantly degrade both the signal-to-noise ratio and the conversion efficiency.

However, multilayer mirror designs covering more than two octaves in bandwidth, which require multi-octave impedance matching, have previously not been achieved. In [65], we recently introduced a dual-adiabatic-matching (DAM) mirror structure, that generates a double chirp not only in the front (as in DCMs) but also in the back section of the mirror approaching the substrate, thus adiabatically tapering the impedance again to provide high transmission for long wavelengths. The front and back chirped high-index layers perform dual adiabatic impedance matching, resulting in (1) high reflectivity and smooth GD over the high-reflectivity range and (2) high transmission with sidelobe suppression outside the high-reflectivity range, respectively.

For a detailed discussion of the mirror design strategy and the SiO_2/TiO_2 multilayer mirror characteristics achieved with such DAM structures, we refer the reader to [65]. Here instead we focus on how these novel mirror structures are actually used in our parametric synthesizer to achieve precise dispersion management over two octaves (see Fig. 7) and we present experimental pulse compression results later in Section II-B.

Fig. 8 shows the reflectivity and dispersion curves (measured with a photospectrometer and a home-built white-light interferometer, respectively) for all GD-ripple-compensated DCM pairs used in the synthesizer. The DCM pairs used in the VIS NOPA and NIR DOPA channels feature extremely smooth GD curves with near-100% reflectivity over their full channel bandwidths. The DCM pair for the IR DOPA channel exhibits a reflectivity >94% up to 2.2 μm, where also the GD starts to oscillate strongly. Unfortunately, this means that with the present NIR DOPA DCM pairs we most probably cannot recompress the amplified spectral components within 2.2–2.5 μm (see Fig. 5). The black curve in Fig. 8 shows the DAM-structure-based ultrabroadband DCM pair [65] used as the final compression unit inside the vacuum chamber. This ultrabroadband DCM pair is designed and optimized for compensating 1.44-mm optical path in fused silica in the spectral range from 0.49 to 1.05 μm (the high-reflectivity range of the DBS1) and 0.32 mm optical path

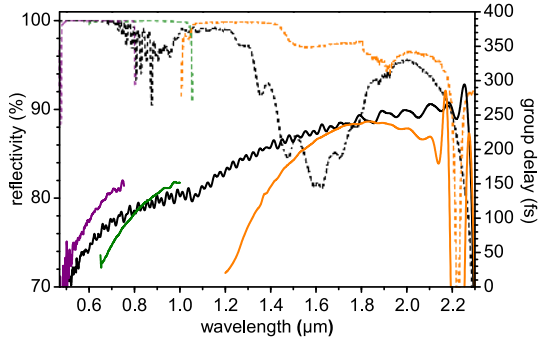

Fig. 8. Reflectivity and GD of all DCM pairs used for dispersion management: total reflectivity (dashed curves) and total GD (solid curves) for a DCM pair used in the VIS NOPA (purple), NIR DOPA (green), and IR DOPA (orange). The black curves show the data for the ultrabroadband DCM pair used for final compression of the combined waveform inside the vacuum chamber; it compensates a 1.44-mm optical path in fused silica and 0.32-mm optical path in ZnSe for ranges of 0.49–1.05 μm and 1.05–2.3 μm, respectively.

in ZnSe from 1.05 to 2.3 μm (the transmission range of DBS1). The total reflectivity of the ultrabroadband DCM pair is >80% and the calculated peak-to-peak values of the average residual GD ripples are controlled to <5 fs over >2-octave bandwidth. The measured dispersion and reflectivity show excellent agreement with the design targets [65].

Because of the resulting smooth transmittance with smooth GD behavior in transmission, a DAM mirror structure can also be used to realize a >2-octave-spanning dispersive chirped dichroic mirror DBS1, as shown in Fig. 9(a) [65]. Note, that the imperfect transmittance around 0.8 μm and the 5% reflection above 1.1 μm are intentionally created to supply the BOC for active feedback stabilization of the relative time delay of the sub-pulses (see Fig. 1). Since the dispersion from the two input ports to the combined output port is matched for this chirped dichroic mirror, the two beams can coherently be combined with very high efficiency >90% over the transition range, even including the ~8% total interface reflection losses resulting from a silica plate in one input port [65].

All ultrabroadband multilayer mirrors, which were grown by ion-beam sputtering, have low absorption losses (<100 ppm). Irradiating our DCMs with 1.5 kW/cm^2 of cw 1030-nm light did not result in any damage from the high average power or in a change in the dispersion. The highest reachable pulse energies, that these multilayer mirrors can handle without damage,

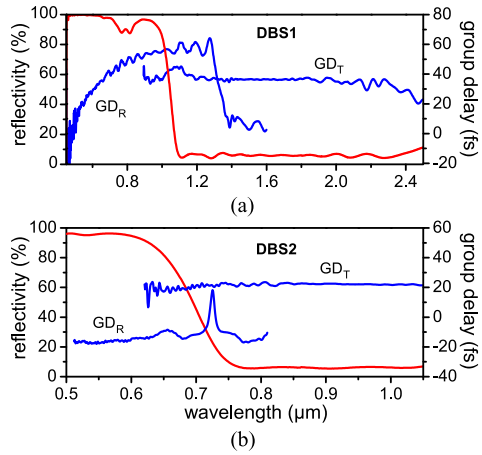

Fig. 9. DBSs: (a) DAM-structure-based >2-octave-spanning chirped DBS/combiner DBS1, (b) dichroic mirror DBS2 used to split/recombine the VIS NOPA and NIR DOPA channels. The red curves show the measured reflectivities, the blue curves the measured group delay in reflection and transmission $GD_{R,T}$.

are determined by the laser-induced damage threshold of the lower bandgap dielectric coating material, TiO_2 in our case. From previous experimental experience, sub-cycle optical waveform synthesizers supporting up to several tens of millijoule of pulse energy with a >1 cm^2 beam size seem feasible based on SiO_2/TiO_2 multilayer chirped mirror technology [65].

The combined waveform, with 1.88-fs TL duration (as computed from the second-stage spectra in Fig. 4), is still chirped when passing through the DBS1 substrate and the CaF_2 vacuum chamber window to decrease the peak intensity and thus reduce the B-integral. Afterwards the ultrabroadband DCM pair can compensate the dispersion of the combined waveform directly before the strong-field experiment. In [65], we evaluated the residual pulse distortions introduced by this compression scheme by considering the measured reflectivity and residual GD errors of the mirrors (i.e., starting from a flat phase and accounting for the measured GD deviation of the mirrors from the design goal, plus the GD in fused silica/ZnSe plates). The analysis revealed that the measured residual phase error of the DCM pair is $<0.1\pi$ rad (i.e., $<\lambda/20$), enabling pulse compression to 1.93-fs duration, i.e., only 3% longer than the TL duration [65]. Thus pulse compression with high fidelity over more than two octaves of bandwidth can be achieved for the first time.

B. Spectro-Temporal Pulse Characterization of Recompressed Channels

Once extremely short and ultrabroadband waveforms are generated, one faces the next paramount challenge: how to perform a complete spectro-temporal characterization of such waveforms in both amplitude and phase? Potential candidates for pulse characterization techniques include frequency-resolved optical gating (FROG), spectral phase interferometry for direct electric field reconstruction (SPIDER), two-dimensional spectral shearing interferometry, and ultimately attosecond ponderomotive streaking [2]. In the end, a combination of several of these techniques and comparison of the results will allow a spectro-temporal characterization excluding potential ambiguities or measurement artifacts.

Here, we present FROG pulse-characterization results of all three second-stage outputs, that demonstrate the feasibility to recompress all three channels simultaneously close to the Fourier limit and show the flexibility of the dispersion management scheme discussed in the previous section for different experimental situations. We emphasize that the FROG results shown in Fig. 10 were measured at the actual waveform synthesis point, i.e., each of the three pulses propagates through its complete synthesizer channel and the beam combiner and thus experiences the correct dispersion and nonlinearity on its way. In other words, the synthesis can later directly be performed from these pulses after locking their relative timing. The VIS NOPA and NIR DOPA were characterized by means of standard SHG-FROG. Because of the octave-spanning bandwidth of the IR DOPA and the spectral coverage of our spectrometer, we opted for surface third-harmonic generation (THG) FROG to characterize the IR DOPA, as this technique is extremely broadband lacking phase-matching constraints.

As discussed in the previous section, the intricate dispersion management scheme employs custom-designed DCM pairs in the individual channels, the chirped dichroic mirrors, plates and wedges (SiO_2, ZnSe) for dispersion fine-tuning and optimization of the seeding conditions in each OPA stage, the CaF_2 window of our future experiment's vacuum chamber, and the ultrabroadband DCM pair as the final compression unit. The FROG reconstructions show that that each of the channels can be compressed close to the TL intensity profile (shown as dashed curves in Fig. 10(d)). In these measurements, we have not yet tried to compress the broadest bandwidths achieved so far (compare broader spectra shown in Fig. 4), so there is some room for further reduction of the pulse durations to $\sim$6 fs for each channel.

The next step will be the final waveform synthesis from the three channels. Since this is ongoing experimental work, we provide in Fig. 11 a few examples of synthesized waveforms for different relative phases computed from the measured spectral amplitudes and phases in Fig. 10(c). Waveforms as short as 2.7 fs FWHM can be obtained.

As in our previous work [56], [57], the different OPA channels need to be combined in a "constant waist width" fashion [66], which is inherently compatible with our OPA synthesis scheme. To this end, the outputs from the different OPA channels are precisely collimated individually with diameters proportional to their carrier wavelengths and then combined on the beam combiners. When finally focused in the attoscience experiment, the three beams in the focus have the same spot size and this "constant waist width" configuration offers the unique property that the temporal pulse form remains unchanged upon propagation, whereas distortions would appear in the near-field when the "constant diffraction length" configuration were used. Fine adjustments of beam divergence can be achieved using adaptive mirrors ([51, Fig. 7(c)]).

Already at the present $\sim$125-μJ-level, our parametric waveform synthesizer spanning more than two octaves provides unprecedented opportunities for strong-field experiments on solids

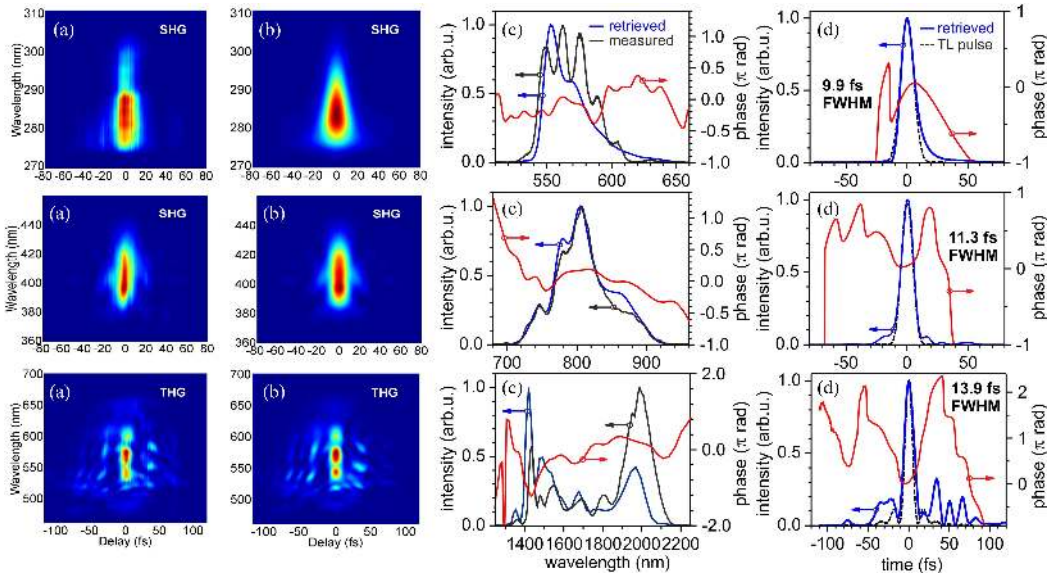

Fig. 10. FROG characterization of the second-stage OPA outputs from the three channels at the synthesis point. The VIS NOPA (top row) and NIR DOPA (middle row) are characterized by means of SHG-FROG, the IR DOPA (bottom row) using surface THG-FROG. (a) Measured and (b) retrieved FROG traces. (c) Measured spectrum, retrieved spectral intensity and phase. (d) Retrieved temporal intensity and phase profiles as well as TL intensity profile. The retrieved FWHM pulse durations are indicated. The reconstruction of the THG-FROG (no marginal correction was applied in this case) shows some deviations from the measured spectrum, since the surface polishing of the ZnSe wedges used for dispersion fine tuning was sub-optimum (scratches and imperfect planarity).

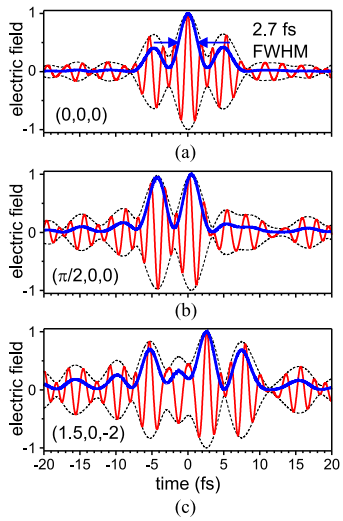

Fig. 11. Synthesized waveforms computed from Fig. 10(c). Field amplitudes of the pulses are the same, phases (VIS NOPA, NIR DOPA, IR DOPA) as indicated. Red: electric field $E(t)$; dashed: field envelope $\tilde{E}(t)$; blue: intensity $I(t)$.

and nanostructured solid-state devices [67]. Our ongoing work aims to recompress and characterize the full three-channel three-stage synthesizer.

C. Passive Timing Jitter Characterization Between Two Channels

So far we have not yet addressed the active feedback stabilization of the relative timing between the three synthesized channels with sub-cycle precision, which is a prerequisite for coherent waveform synthesis. In previous works by Leitenstorfer's group [68], [69], attosecond-level passive relative timing jitter between two channels of a nanojoule-level waveform synthesizer based on erbium-doped fiber technology was demonstrated. Our own earlier experiments [56]–[58] demonstrated coherent waveform synthesis on the microjoule level already. Here we present the first study of the passive timing jitter properties of a scaled-up multimillijoule sub-cycle waveform synthesizer, which has a much longer beam path (∼30 meters) compared to those earlier synthesizers. Our results reveal a high passive timing stability between the synthesized channels, which corroborates the feasibility to actually perform the coherent synthesis after making some improvements on the feedback stabilization.

As shown in Fig. 1, we spatially and temporally combined the three OPA pulses after the third amplification stages (VIS NOPA3, NIR DOPA3, IR DOPA3) on the dichroic beam combiners discussed in Section II-A. As already mentioned, the dichroic mirrors feature a ∼5% leakage composed of the combined OPA pulses collinear with each other, which is used to supply the BOC setups. We first implemented the BOC for VIS NOPA3 and IR DOPA3, the setup is similar to the one shown in Fig. 9 in [2]: the BOC consists of two identical cross-correlators, in which the 580-nm component from the VIS NOPA3 and the 1550-nm component from IR DOPA3 generate the sum frequency at 420 nm, in two 1-mm-thick type-I BBO crystals. A 3-mm-thick glass plate is inserted in one of the cross-correlators, to reverse the time order of the two pulses. The sum-frequency signals are filtered within a 10-nm optical bandwidth in front of the home-built balanced photodetector (for details see [70]). The IR pulses are used as the reference, and we use a piezo-transducer (PZT) actuated delay stage in the VIS channel to compensate for the relative timing jitter.

In Fig. 12, we report the first characterization data of the natural (i.e., passive, unstabilized) timing jitter between the VIS NOPA3 and IR DOPA3 outputs in our multimillijoule waveform

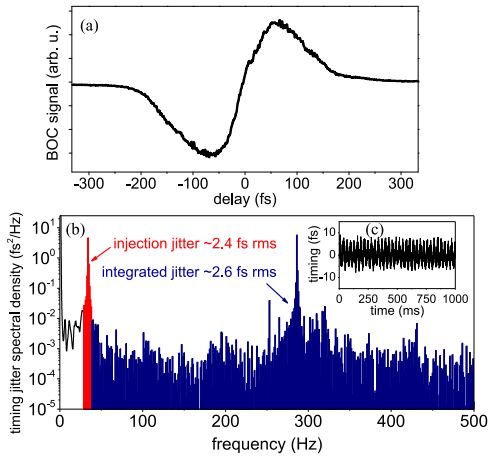

Fig. 12. Passive timing jitter characterization: (a) BOC S-curve for VIS NOPA3 and IR DOPA3, exhibiting a ∼100-fs wide linear region useful for feedback stabilization. (b) Natural timing jitter spectral density between the two channels measured by the same BOC. The red area corresponds to the injected sinusoidal test signal with ∼2.4-fs rms jitter at 33.3 Hz, while the blue area corresponds to the natural (i.e., passive, unstabilized) timing jitter. By comparison with the injected signal peak, the natural timing jitter is evaluated to be only ∼2.6 fs rms. The inset (c) shows the same BOC signal in the time domain with the clear modulation from the injected 33.3-Hz test signal.

synthesizer [70]. The typical S-shaped BOC signal displayed in Fig. 12(a) features a ∼100-fs wide linear region, which can directly be used for feedback stabilization of the relative timing. For the moment, to investigate the noise properties and to evaluate the overall passive timing stability of the system, we used the following experimental procedure: we injected a known sinusoidal signal at 33.3 Hz, with 1-V peak-to-peak amplitude driving the PZT used for adjusting the relative timing. From the specifications of the PZT, we calibrated the rms of this injected sinusoidal signal to be ∼2.4 fs. Afterwards, by comparing the red area in Fig. 12(b) corresponding to the known injected noise to the blue area corresponding to the passive timing jitter, we could evaluate the overall timing jitter to be ∼2.6 fs rms. Note that the PZT-based feedback stabilization can easily eliminate the low-frequency timing jitter. Unfortunately, in this first experiment we observed that the injected 33.3-Hz signal driving the PZT excited a resonance in the PZT giving rise to the broad noise band from 250 to 330 Hz visible in Fig. 12(b). We expect to get rid of this excessive high-frequency noise by simply replacing the PZT in future experiments. Together with improved vibration isolation and environmental shielding of the BOC setup we expect to achieve a sub-cycle timing lock soon.

Apart from the PZT-resonance issue, the observed surprisingly low ∼2.6-fs rms jitter seems a direct consequence of our parallel synthesizer architecture, in which all three channels are seeded by a *common* CEP-stable supercontinuum generated in a YAG plate. On a second-time-scale, the passive stability of our setup is sufficient to guarantee already a few-femtosecond timing stability. In contrast, if the channels were seeded by different white-light supercontinua created from separate pulses with uncorrelated pulse-energy fluctuations, a substantial timing jitter [71] between the synthesizer channels could occur.

To summarize, the timing jitter between parallel OPA channels in our synthesizer is already at the level of 1–2 optical cycles without any active stabilization. Replacing the PZT and improving the vibration isolation and environmental shielding of the BOC setup should enable locking of the different sub-pulses well below a tenth if not a hundredth of a cycle.

III. Waveform Synthesis Based on Two-Color-Driven Gas-Filled HCF

In Section I, we already mentioned that waveform synthesis based on SPM in a neon-filled HCF compressor recently allowed the generation of sub-cycle optical pulses [3], [51], [52]. If one intends to pursue the synthesis of the *shortest possible* waveforms within this scheme, it is first necessary to equalize the ultrabroadband spectrum: since the UV channel contains the smallest pulse energy [3], [51], [52], it contributes to the resulting pulse duration only if the predominant longer-wavelength regions close to the Ti:sapphire driver wavelengths are adequately suppressed. This limits the total output energy of the multi-channel synthesizer to a few tens of microjoules. However, the resulting reduction in pulse energy to a few tens of microjoules then limits the usefulness of this source and unfortunately precludes many interesting applications in attoscience. A potential solution out of this dilemma is the application of induced-phase modulation (IPM) [72], [73] based on the interaction between two (or more) copropagating optical pulses of different color and relatively long pulse duration in a gas-filled HCF. The IPM technique, sketched in Fig. 13, offers control over the spectral shape of the HCF supercontinuum by adjusting the relative intensity ratio and the temporal delay Δt between the input pulses and allows a more efficient generation of ultrabroadband optical pulses than those produced solely by SPM [3], [51], [52]. Such an IPM-based synthesizer (see Fig. 13) is expected to greatly relieve the energy-scaling bottleneck in the UV region [52], and the enhanced spectral broadening of the UV region (compare Fig. 14) is particularly appealing for the realization of ultrahigh HHG conversion efficiencies in bright tabletop HHG sources [54]. By employing the advantages of IPM, the Yamashita group (Hokkaido University, Sapporo, Japan) has previously demonstrated an isolated 1.3-cycle pulse with 2.6-fs duration and 3.6-μJ energy centered at 600 nm [72]. Later, much broader spectra (270–1000 nm) with several hundred microjoules were generated, supporting the generation of 1.5-fs pulses [73]. Pushing the pulse energy to the millijoule level would have a tremendous impact for applications in attoscience and strong-field physics.

In this section, we discuss our recent experimental progress toward an above-millijoule IPM waveform synthesizer [74], [75] driven by a CEP-stabilized Ti:sapphire chirped-pulse amplification (CPA) system. Using a neon-filled fused-silica HCF, we obtained a 1.72-mJ CEP-locked supercontinuum spanning the range 340–950 nm, which is straightforwardly compressible to terawatt attosecond optical waveforms.

The setup shown in Fig. 13 provides details of our experiment. The output beam of an 800-nm, 30-fs, 5.5-mJ CEP-stabilized Ti:sapphire CPA system with a 3 kHz repetition rate was divided into two beams by a beam splitter (BS) with a splitting ratio of 55:45 (reflectance:transmittance). The reflected pulses were used as fundamental pulses (ω). The transmitted pulses

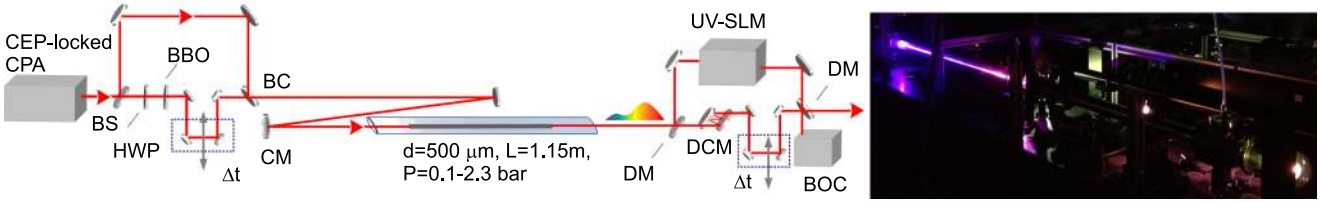

Fig. 13. (Left) Optical waveform synthesizer based on IPM in a two-color-driven gas-filled HCF compressor: BS, beam splitter; BBO, β-barium borate crystal; HWP, half-wave plate; BC, beam combiner; CM, concave mirror; DM, dichroic mirror; DCM, double-chirped mirror; UV-SLM, UV spatial light modulator; BOC, balanced optical cross-correlator. (Right) Photo of the experiment. The red and blue input pulses are visible on the left, the white-light supercontinuum can be seen (partly obstructed) on the right.

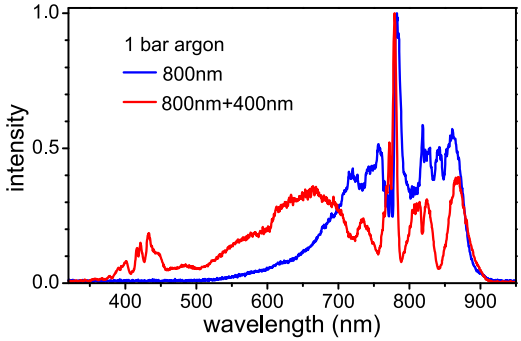

Fig. 14. Comparison of single- versus two-color-driven HCF supercontinuum using 1 bar argon: blue curve, single color [$E_{\rm in} = 480\ \mu$J at 800 nm, $E_{\rm out} = 340\ \mu$J]; red curve, two colors [$E_{\rm in} = 800\ \mu$J at 800 nm + 60 μJ at 400 nm, $E_{\rm out} = 380\ \mu$J (in the fundamental mode)]. The enhanced spectral broading at shorter wavelengths due to IPM compared to the pure SPM case is evident.

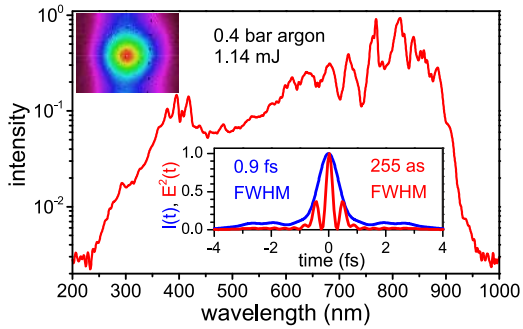

Fig. 15. Supercontinuum with 1.14 mJ energy from 0.4 bar argon. The inset shows the TL intensity profile $I(t)$ (blue trace) indicating a 0.9-fs TL pulse duration and the TL $E^2(t)$ profile (red trace). Input pulse energies $E_{800\,\rm nm} =$ 1.72 mJ, $E_{400\,\rm nm} =$ 0.9 mJ, output $E_{\rm out} =$ 1.14 mJ. The inset on the top left exhibits a nice output beam profile, the five black spots are a measurement artifact.

passed through a half-wave plate (HWP), followed by a 0.5-mm-thick type-I BBO crystal to generate the second-harmonic (2ω) pulses at 400 nm with the same polarization as the reflected pulses at 800 nm. Two pairs of harmonic separators were used to filter out the residual fundamental pulses from the second-harmonic pulses, as well as to adjust the delay Δt for optimum IPM. The ω and 2ω pulses were recombined using a dichroic mirror and reflected by a concave silver mirror with an (experimentally determined) focal length $f = 190$ cm, which focused the combined beam into a fused-silica HCF (length $L = 115$ cm, diameter $d = 500\ \mu$m). The fiber was placed in the middle of a 400-cm-long glass tube sealed at the two ends with 3-mm-thick CaF_2 windows at Brewster angle. Also in this system, two active beam-pointing stabilization units (not shown in Fig. 13) before and after the HCF setup are used to achieve reliable input and output coupling required for long-term stable operation.

Fig. 15 reports a HCF supercontinuum with 1.14-mJ output energy, 0.9-fs TL duration and good output beam profile from 0.4 bar argon. The inset in Fig. 15 also displays the TL $E^2(t)$ profile, which exhibits an isolated 255-as FWHM short central spike, that is expected to determine light-matter interactions in strong-field attoscience experiments.

To obtain the HCF output with broadest supercontinuum and highest energy, a fundamental pulse with 2.3-mJ energy and a second-harmonic pulse with 0.42-mJ energy were focused and injected into the HCF filled with neon at 2.3 bar pressure. Fig. 16 shows this 1.72-mJ HCF output spectrum (covering 365–930 nm, measured at 1% of the peak intensity) supporting 0.9-fs TL pulses.

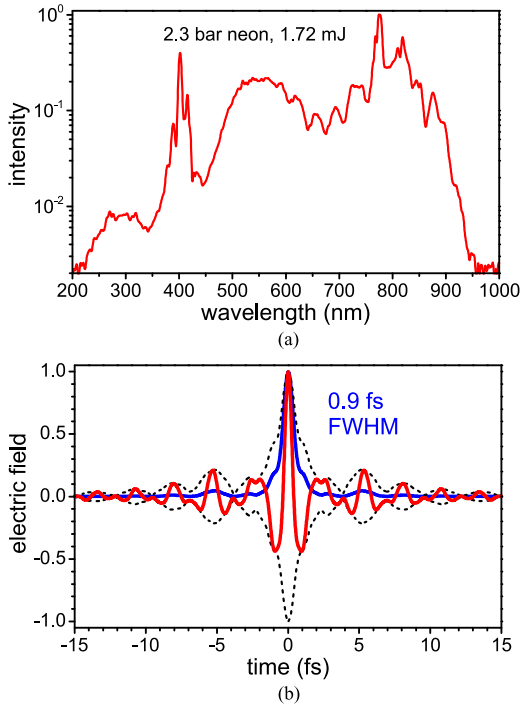

Fig. 16. (a) Supercontinuum with 1.72 mJ energy from 2.3 bar neon. Input pulse energies $E_{800\,\rm nm} = 2.3$ mJ, $E_{400\,\rm nm} = 0.42$ mJ, output $E_{\rm out} = 1.72$ mJ. (b) Corresponding TL electric field $E(t)$ (red trace), TL envelope $\tilde{E}(t)$ (dashed traces), TL intensity profile $I(t)$ (blue trace) indicating a 0.9-fs FWHM TL duration.

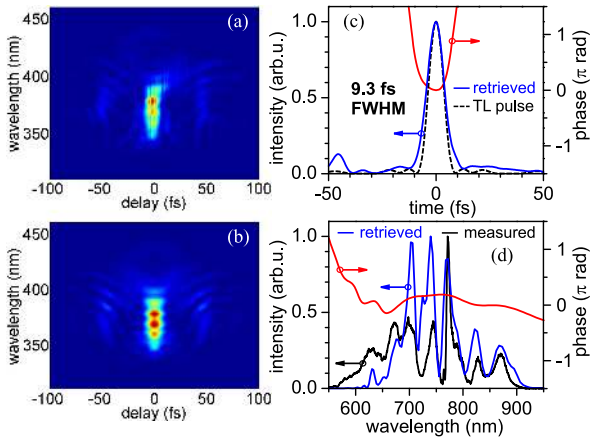

Fig. 17. SHG-FROG characterization of a narrowband NIR channel (660–1000 nm): (a) Measured and (b) retrieved FROG traces. (c) FROG retrieved temporal intensity and phase profiles as well as TL intensity profile. (d) Measured spectrum, FROG retrieved spectral intensity and phase.

As indicated in the experimental setup shown in Fig. 13, the created supercontinuum is split into two parallel wavelength channels. The longer-wavelength part will be compressed by custom-designed DCMs, that are currently being designed. The short-wavelength part will be compressed by a UV spatial light modulator (SLM). This 648-pixel, 2D SLM featuring a transmittance of $>85\%$ in the wavelength region from 260 to 1100 nm [76], [77] was successfully used in earlier experiments by the Yamashita group to compress IPM supercontinua down to 1.3-cycle pulse with 2.6-fs duration [72]. As done in the parametric synthesizer discussed earlier in Section II, we will finally perform the waveform synthesis recombining the two channels using a broadband dichroic mirror and tightly locking the relative timing between the sub-pulses using the BOC technique.

Experiments on the compression of the complete supercontinuum bandwidth using newly designed broadband DCMs and the UV SLM are in progress. Here, we present preliminary SHG-FROG pulse-characterization results (see Fig. 17) of the NIR channel using Ti:sapphire-oscillator DCMs, that were available at the moment. The dispersion compensation scheme includes Ti:sapphire DCM pairs (covering only the narrow region 660–1000 nm), plates and wedges (SiO_2) for dispersion fine-tuning, and the CaF_2 window of our experiment's vacuum chamber. The preliminary SHG-FROG data yield compressed 9.3-fs pulses very close to the 8-fs TL for this narrowband channel.

IV. Summary

In this paper we have discussed two alternative technological routes toward CEP-stable multimillijoule sub-cycle optical waveform synthesis based on (1) parametric amplification and (2) IPM in a two-color-driven gas-filled HCF compressor. We have addressed the challenges and presented the experimental toolbox needed to generate and characterize stable sub-cycle waveforms with multimillijoule energies. The presented CEP-stable multimillijoule three-channel parametric waveform synthesizer aiming to generate $\sim$1.9-fs FWHM waveforms with >2 mJ energy demonstrates the game-changing capability to overcome the traditional bandwidth limitations of ultrafast amplifiers, such as CPAs, OPAs and OPCPAs. It can therefore be regarded as first incarnation of a prototype sub-cycle parametric synthesizer architecture, that can later directly be transferred to Yb-doped pump-laser technology, in particular cryogenically cooled, Innoslab, or thin-disk laser technology [2], to overcome pulse-energy and average-power bottlenecks in the near future. This technology is therefore very attractive for various applications in next-generation light sources such as SLAC, European XFEL, SACLA, FERMI and ELI-ALPS, targeting extreme operation parameter regimes. Second, we have also discussed the generation of CEP-stable 1.72-mJ waveforms using IPM in a two-color-driven gas-filled HCF. These waveforms are expected to be straightforwardly compressible close to the 0.9-fs FWHM Fourier limit with a 255-as FWHM short central spike in the $E^2(t)$ profile, that governs light-matter interactions in strong-field attoscience experiments. We foresee that these novel sources will soon become versatile tools for controlling strong-field interactions in atoms, molecules, solids and nanostructures, and for attosecond pump-probe spectroscopy employing ultrashort pulses in the VIS/IR and XUV/soft-X-ray regions.

Acknowledgment

S. Fang thanks Prof. Mikio Yamashita for UV-SLM fabrication and discussions.

References

[1] G. M. Rossi *et al.*, "Spectrotemporal characterization of all channels in a sub-optical-cycle parametric waveform synthesizer," presented at the Conf. Laser Electro-Optics, San Jose, CA, USA, 2014, Paper SF1E.3.
[2] C. Manzoni *et al.*, "Coherent pulse synthesis: Towards sub-cycle optical waveforms," *Laser Photon. Rev.*, vol. 9, pp. 129–171, 2015.
[3] A. Wirth *et al.*, "Synthesized light transients," *Science*, vol. 334, pp. 195–200, 2011.
[4] F. Krausz and M. Ivanov, "Attosecond physics," *Rev. Mod. Phys.*, vol. 81, pp. 163–234, 2009.
[5] E. J. Takahashi, P. Lan, O. D. Mücke, Y. Nabekawa, and K. Midorikawa, "Infrared two-color multicycle laser field synthesis for generating an intense attosecond pulse," *Phys. Rev. Lett.*, vol. 104, p. 233901, 2010.
[6] E. J. Takahashi, P. Lan, O. D. Mücke, Y. Nabekawa, and K. Midorikawa, "Attosecond nonlinear optics using gigawatt-scale isolated attosecond pulses," *Nature Commun.*, vol. 4, p. 2691, 2013.
[7] G. Sansone, L. Poletto, and M. Nisoli, "High-energy attosecond light sources," *Nature Photon.*, vol. 5, pp. 655–663, 2011.
[8] M. Kolesik, J. M. Brown, J. V. Moloney, and D. Faccio, "History-dependent effects in subcycle-waveform strong-field ionization," *Phys. Rev. A*, vol. 90, p. 033414, 2014.
[9] L. E. Chipperfield, J. S. Robinson, J. W. G. Tisch, and J. P. Marangos, "Ideal waveform to generate the maximum possible electron recollision energy for any given oscillation period," *Phys. Rev. Lett.*, vol. 102, p. 063003, 2009.
[10] J. A. Pérez-Hernández, M. F. Ciappina, M. Lewenstein, L. Roso, and A. Zaïr, "Beyond carbon K-edge harmonic emission using a spatial and temporal synthesized laser field," *Phys. Rev. Lett.*, vol. 110, p. 053001, 2013.
[11] C. Jin, G. Wang, H. Wei, A.-T. Le, and C. D. Lin, "Waveforms for optimal sub-keV high-order harmonics with synthesized two- or three-colour laser fields," *Nature Commun.*, vol. 5, p. 4003, 2014.
[12] C. Jin, G. Wang, H. Wei, A.-T. Le, and C. D. Lin, "Route to optimal generation of soft X-ray high harmonics with synthesized two-color laser pulses," *Sci. Rep.*, vol. 4, p. 7067, 2014.
[13] S. Haessler *et al.*, "Optimization of quantum trajectories driven by strong-field waveforms," *Phys. Rev. X*, vol. 4, p. 021028, 2014.
[14] E. Balogh *et al.*, "Genetic optimization of attosecond-pulse generation in light-field synthesizers," *Phys. Rev. A*, vol. 90, p. 023855, 2014.
[15] L. Veisz *et al.*, "Generation and applications of sub-5-fs multi-10-TW light pulses," presented at the Conf. Lasers Electro-Optics Pacific Rim, Kyoto, Japan, 2013, Paper TuD2_3.

[16] M. R. Edwards, V. T. Platonenko, and J. M. Mikhailova, "Enhanced attosecond bursts of relativistic high-order harmonics driven by two-color fields," *Opt. Lett.*, vol. 39, pp. 6823–6826, 2014.

[17] S. P. D. Mangles *et al.*, "Monoenergetic beams of relativistic electrons from intense laser-plasma interactions," *Nature*, vol. 431, pp. 535–538, 2004.

[18] C. G. R. Geddes *et al.*, "High-quality electron beams from a laser wakefield accelerator using plasma-channel guiding," *Nature*, vol. 431, pp. 538–541, 2004.

[19] J. Faure *et al.*, "A laser-plasma accelerator producing monoenergetic electron beams," *Nature*, vol. 431, pp. 541–544, 2004.

[20] A. Buck *et al.*, "Real-time observation of laser-driven electron acceleration," *Nature Phys.*, vol. 7, pp. 543–548, 2011.

[21] W. P. Leemans *et al.*, "Multi-GeV electron beams from capillary-discharge-guided subpetawatt laser pulses in the self-trapping regime," *Phys. Rev. Lett.*, vol. 113, p. 245002, 2014.

[22] S. Chen *et al.*, "MeV-energy X rays from inverse Compton scattering with laser-wakefield accelerated electrons," *Phys. Rev. Lett.*, vol. 110, p. 155003, 2013.

[23] S. Corde *et al.*, "Femtosecond x rays from laser-plasma accelerators," *Rev. Mod. Phys.*, vol. 85, pp. 1–48, 2013.

[24] M. Krüger, M. Schenk, and P. Hommelhoff, "Attosecond control of electrons emitted from a nanoscale metal tip," *Nature*, vol. 475, pp. 78–81, 2011.

[25] G. Herink, D. R. Solli, M. Gulde, and C. Ropers, "Field-driven photoemission from nanostructures quenches the quiver motion," *Nature*, vol. 483, pp. 190–193, 2012.

[26] B. Piglosiewicz *et al.*, "Carrier-envelope phase effects on the strong-field photoemission of electrons from metallic nanostructures," *Nature Photon.*, vol. 8, pp. 37–42, 2014.

[27] M. Gulde *et al.*, "Ultrafast low-energy electron diffraction in transmission resolves polymer/graphene superstructure dynamics," *Science*, vol. 345, pp. 200–204, 2014.

[28] O. D. Mücke, T. Tritschler, M. Wegener, U. Morgner, and F. X. Kärtner, "Signatures of carrier-wave Rabi flopping in GaAs," *Phys. Rev. Lett.*, vol. 87, p. 057401, 2001.

[29] O. D. Mücke, T. Tritschler, M. Wegener, U. Morgner, and F. X. Kärtner, "Role of the carrier-envelope offset phase of few-cycle pulses in nonperturbative resonant nonlinear optics," *Phys. Rev. Lett.*, vol. 89, p. 127401, 2002.

[30] O. D. Mücke, T. Tritschler, M. Wegener, U. Morgner, and F. X. Kärtner, "Determining the carrier-envelope offset frequency of 5-fs pulses with extreme nonlinear optics in ZnO," *Opt. Lett.*, vol. 27, pp. 2127–2129, 2002.

[31] T. Tritschler, O. D. Mücke, M. Wegener, U. Morgner, and F. X. Kärtner, "Evidence for third-harmonic generation in disguise of second-harmonic generation in extreme nonlinear optics," *Phys. Rev. Lett.*, vol. 90, p. 217404, 2003.

[32] Q. T. Vu *et al.*, "Light-induced gaps in semiconductor band-to-band transitions," *Phys. Rev. Lett.*, vol. 92, p. 217403, 2004.

[33] O. D. Mücke, T. Tritschler, and M. Wegener, "Resonant nonperturbative extreme nonlinear optics with two-cycle pulses: Carrier-wave Rabi flopping and role of the carrier-envelope offset phase," in *Few-Cycle Laser Pulse Generation and Its Applications*. F. X. Kärtner, Ed. Berlin, Germany: Springer, 2004, pp. 379–410.

[34] Y. H. Wang, H. Steinberg, P. Jarillo-Herrero, and N. Gedik, "Observation of Floquet-Bloch states on the surface of a topological insulator," *Science*, vol. 342, pp. 453–457, 2013.

[35] A. H. Chin, J. M. Bakker, and J. Kono, "Ultrafast electroabsorption at the transition between classical and quantum response," *Phys. Rev. Lett.*, vol. 85, pp. 3293–3296, 2000.

[36] S. Ghimire *et al.*, "Redshift in the optical absorption of ZnO single crystals in the presence of an intense midinfrared laser field," *Phys. Rev. Lett.*, vol. 107, p. 167407, 2011.

[37] M. Schultze *et al.*, "Attosecond band-gap dynamics in silicon," *Science*, vol. 346, pp. 1348–1352, 2014.

[38] S. Ghimire *et al.*, "Observation of high-order harmonic generation in a bulk crystal," *Nature Phys.*, vol. 7, pp. 138–141, 2011.

[39] O. D. Mücke, "Isolated high-order harmonics pulse from two-color-driven Bloch oscillations in bulk semiconductors," *Phys. Rev. B*, vol. 84, p. 081202(R), 2011.

[40] A. Schiffrin *et al.*, "Optical-field-induced current in dielectrics," *Nature*, vol. 493, pp. 70–74, 2013.

[41] M. Schultze *et al.*, "Controlling dielectrics with the electric field of light," *Nature*, vol. 493, pp. 75–78, 2013.

[42] R. Ell *et al.*, "Generation of 5-fs pulses and octave-spanning spectra directly from a Ti:sapphire laser," *Opt. Lett.*, vol. 26, pp. 373–375, 2001.

[43] M. Nisoli *et al.*, "Generation of high energy 10 fs pulses by a new pulse compression technique," *Opt. Lett.*, vol. 22, pp. 522–524, 1997.

[44] A. Baltuška, Z. Wei, M. S. Pshenichnikov, and D. A. Wiersma, "Optical pulse compression to 5 fs at a 1-MHz repetition rate," *Opt. Lett.*, vol. 22, pp. 102–104, 1997.

[45] O. D. Mücke *et al.*, "Self-compression of millijoule 1.5 μm pulses," *Opt. Lett.*, vol. 34, pp. 2498–2500, 2009.

[46] C. P. Hauri *et al.*, "Generation of intense, carrier-envelope phase-locked few-cycle laser pulses through filamentation," *Appl. Phys. B*, vol. 79, pp. 673–677, 2004.

[47] C. P. Hauri *et al.*, "Generation of intense few-cycle laser pulses through filamentation—Parameter dependence," *Opt. Exp.*, vol. 13, pp. 7541–7547, 2005.

[48] G. Stibenz, N. Zhavoronkov, and G. Steinmeyer, "Self-compression of millijoule pulses to 7.8 fs duration in a white-light filament," *Opt. Lett.*, vol. 31, pp. 274–276, 2006.

[49] A. Baltuška, T. Fuji, and T. Kobayashi, "Visible pulse compression to 4 fs by optical parametric amplification and programmable dispersion control," *Opt. Lett.*, vol. 27, pp. 306–308, 2002.

[50] D. Brida *et al.*, "Few-optical-cycle pulses tunable from the visible to the mid-infrared by optical parametric amplifiers," *J. Opt.*, vol. 12, p. 013001, 2010.

[51] M. T. Hassan *et al.*, "Attosecond photonics: Synthesis and control of light transients," *Rev. Sci. Instrum.*, vol. 83, p. 111301, 2012.

[52] T. T. Luu *et al.*, "Isolated optical attosecond pulses," presented at the Conf. Lasers Electro-Optics, San Jose, CA, USA, 2013, Paper QF1C.6.

[53] E. J. Takahashi, T. Kanai, K. L. Ishikawa, Y. Nabekawa, and K. Midorikawa, "Coherent water window X ray by phase-matched high-order harmonic generation in neutral media," *Phys. Rev. Lett.*, vol. 101, p. 253901, 2008.

[54] T. Popmintchev *et al.*, "Bright coherent ultrahigh harmonics in the keV X-ray regime from mid-infrared femtosecond lasers," *Science*, vol. 336, pp. 1287–1291, 2012.

[55] A. Harth *et al.*, "Two-color pumped OPCPA system emitting spectra spanning 1.5 octaves from VIS to NIR," *Opt. Exp.*, vol. 20, pp. 3076–3081, 2012.

[56] S.-W. Huang *et al.*, "High-energy pulse synthesis with sub-cycle waveform control for strong-field physics," *Nature Photon.*, vol. 5, pp. 475–479, 2011.

[57] S.-W. Huang *et al.*, "Optical waveform synthesizer and its application to high-harmonic generation," *J. Phys. B*, vol. 45, p. 074009, 2012.

[58] C. Manzoni *et al.*, "Coherent synthesis of ultra-broadband optical parametric amplifiers," *Opt. Lett.*, vol. 37, pp. 1880–1882, 2012.

[59] B. E. Schmidt *et al.*, "Frequency domain optical parametric amplification," *Nature Commun.*, vol. 5, p. 3643, 2014.

[60] G. Cirmi *et al.*, "Towards parametric synthesis of millijoule-level two-octave-wide optical waveforms for strong-field experiments," presented at the Conf. Ultrafast Opt., 2013, Davos, Switzerland, Paper We3.3.

[61] O. D. Mücke *et al.*, "Millijoule-level parametric synthesizer generating two-octave-wide optical waveforms for strong-field experiments," presented at the Conf. Lasers Electro-Optics, San Jose, CA, USA, 2013, Paper CTh3H.3.

[62] S. Fang *et al.*, "Multi-mJ parametric synthesizer generating two-octave-wide optical waveforms," presented at the Conf. Laser Electro-Optics Pacific Rim, Kyoto, Japan, 2013, Paper WB3-1.

[63] G. Cerullo, A. Baltuška, O. D. Mücke, and C. Vozzi, "Few-optical-cycle light pulses with passive carrier-envelope phase stabilization," *Laser Photon. Rev.*, vol. 5, pp. 323–351, 2011.

[64] J. Moses, C. Manzoni, S.-W. Huang, G. Cerullo, and F. X. Kärtner, "Temporal optimization of ultrabroadband high-energy OPCPA," *Opt. Exp.*, vol. 17, pp. 5540–5555, 2009.

[65] S.-H. Chia *et al.*, "Two-octave-spanning dispersion-controlled precision optics for sub-optical-cycle waveform synthesizers," *Optica*, vol. 1, pp. 315–322, 2014.

[66] Q. Zou and B. Lü, "Propagation properties of ultrashort pulsed beams with constant waist width in free space," *Opt. Laser Technol.*, vol. 39, pp. 619–625, 2007.

[67] P. D. Keathley *et al.*, "Strong-field photoemission from silicon field emitter arrays," *Ann. Phys.*, vol. 525, pp. 144–150, 2013.

[68] F. Adler, A. Sell, F. Sotier, R. Huber, and A. Leitenstorfer, "Attosecond relative timing jitter and 13 fs tunable pulses from a two-branch Er:fiber laser," *Opt. Lett.*, vol. 32, pp. 3504–3506, 2007.

[69] G. Krauss *et al.*, "Synthesis of a single cycle of light with compact erbium-doped fibre technology," *Nature Photon.*, vol. 4, pp. 33–36, 2010.
[70] R. Mainz *et al.*, "Timing jitter characterization of a high-energy sub-cycle optical waveform synthesizer," presented at the Conf. Advanced Solid State Lasers, Shanghai, China, 2014, Paper ATu5A.3.
[71] C. Manzoni, G. Cirmi, D. Brida, S. De Silvestri, and G. Cerullo, "Optical-parametric-generation process driven by femtosecond pulses: Timing and carrier-envelope phase properties," *Phys. Rev. A*, vol. 79, p. 033818, 2009.
[72] E. Matsubara, K. Yamane, T. Sekikawa, and M. Yamashita, "Generation of 2.6 fs optical pulses using induced-phase modulation in a gas-filled hollow fiber," *J. Opt. Soc. Am. B*, vol. 24, pp. 985–989, 2007.
[73] S. Fang *et al.*, "Generation of sub-900-μJ supercontinuum with a two-octave bandwidth based on induced phase modulation in argon-filled hollow fiber," *IEEE Photon. Technol. Lett.*, vol. 23, pp. 688–690, 2011.
[74] S. Fang *et al.*, "High-energy carrier-envelope phase-stable optical waveforms compressible to <1 fs using induced-phase modulation in argon-filled hollow-core fiber," presented at the Conf. High-Intensity Lasers and High-Field Phenomena, Berlin, Germany, 2014, Paper HW1C.2.
[75] S. Fang *et al.*, "Above-millijoule optical waveforms compressible to sub-fs using induced-phase modulation in a neon-filled hollow-core fiber," presented at the Conf. Ultrafast Phenomena, Okinawa, Japan, 2014, Paper 09.Wed.P3.60.
[76] T. Tanigawa, Y. Sakakibara, S. Fang, T. Sekikawa, and M. Yamashita, "Spatial light modulator of 648 pixels with liquid crystal transparent from ultraviolet to near-infrared and its chirp compensation application," *Opt. Lett.*, vol. 34, pp. 1696–1698, 2009.
[77] K. Yamane, M. Katayose, and M. Yamashita, "Spectral phase characterization of two-octave bandwidth pulses by two-dimensional spectral shearing interferometry based on noncollinear phase matching with external pulse pair," *IEEE Photon. Technol. Lett.*, vol. 23, pp. 1130–1132, 2011.

Oliver D. Mücke received the Diploma and Ph.D. degrees in physics from Universität Karlsruhe, Karlsruhe, Germany, in 1999 and 2003, respectively. From 2003 to 2007, he was a Feodor Lynen Fellow of the Alexander von Humboldt Foundation and later a Postdoctoral Associate with the MIT Research Laboratory of Electronics. In 2007, he joined the Photonics Institute at the Vienna University of Technology, Vienna, Austria, supported by a FWF Lise Meitner Senior Postdoc Fellowship (09/2008–09/2010). Since July 2011, he has been a Senior Scientist at DESY CFEL, Hamburg, Germany. His research interests include CEP-stable few-cycle pulse generation from octave-spanning Ti:sapphire oscillators and parametric amplifiers, high-energy multioctave waveform synthesis, strong-field physics and attoscience, highly efficient intense terahertz-pulse generation, laser-driven sources of particles and hard-X-rays, frequency-comb technology for optical clocks, and extreme nonlinear optics in solids and nanostructures.

Shaobo Fang received the bachelor's degree from Tianjin University, Tianjin, China, and the Ph.D. degree from Hokkaido University, Sapporo, Japan. From 2007 to 2011, he was an Assistant Research Scientist of the Core Research for Evolutional Science and Technology, Japan Science and Technology Agency. Since 2011, he has been a Research Scientist in the framework of the Helmholtz Association Young Scientist Program at DESY CFEL, Hamburg, Germany. His research interests include sub-cycle waveform synthesis and novel mono-cycle pulse generation for attosecond science and compact X-ray sources.

Giovanni Cirmi received the bachelor's and master's degrees in electrical engineering in 2003 and 2005, respectively, and the Ph.D. degree in physics from Politecnico di Milano, Milan, Italy, in 2009. He was a Postdoctoral Fellow and a Postdoctoral Associate with the Massachusetts Institute of Technology, Cambridge, MA, USA, with a fellowship from Progetto Rocca and another from AFOSR. He is currently a Research Scientist at DESY CFEL, Hamburg, Germany. His main research interests include high-energy few-cycle optical pulses in the femtosecond regime generated via optical parametric (chirped pulse) amplification and in the attosecond regime via high-harmonic generation, pulse synthesis of few-cycle pulses, carrier-envelope phase stabilization, ultrafast spectroscopy on femtosecond and attosecond time scales.

Giulio Maria Rossi received the bachelor's and master's degrees in physics engineering from Politecnico di Milano, Milan, Italy, in 2011 and 2013, respectively. During that time, his research was on parametric amplifiers, pulse characterization techniques, and ultrafast pump–probe spectroscopy. His current research interests include sub-cycle waveform synthesizers and attosecond pulse generation.

Shih-Hsuan Chia received the bachelor's and master's degrees from National Taiwan University, Taipei, Taiwan, in 2007 and 2009, respectively. His research interests include femtosecond laser dynamics, nonlinear fiber optics, and nonlinear light microscopy. His current research interests include dispersion management and chirped mirror designs for sub-cycle waveform synthesizers.

Hong Ye received the master's degree in applied physics from Chalmers University of Technology, Gothenburg, Sweden, in 2011. Since 2012 until she joined DESY CFEL, she had been working on light emission from semiconductor materials. Her current research interests include two-color-driven gas-filled hollow-core fiber pulse compression and coherent electron beams from field-emitter arrays using solid-state velocity map imaging.

Yudong Yang received the bachelor's degree from Sun Yat-Sen University, Guangzhou, China, in 2009, and the master's degree from Peking University, Beijing, China, in 2012. His current research at DESY CFEL, Hamburg, Germany, is focused on HHG and attoscience.

Roland Mainz received the bachelor's and Diploma degrees in physics from the University of Rostock, Rostock, Germany, in 2010 and 2013, respectively. His research interests include HHG, its application and control, pulsed sources for attoscience, attosecond metrology, and ultrafast spectroscopy.

Cristian Manzoni received the Ph.D. degree in physics from the Physics Department, Politecnico di Milano, Milan, Italy, where he focused on passive carrier-envelope phase stabilization and time-resolved spectroscopy of nanostructures. From 2006 to 2009, his Postdoctoral research concerned the generation of broadband IR pulses, spectral phase control, and nonlinear processes in poled crystals. In 2009, he joined the Max Planck Research Group for Structural Dynamics with the Center for Free-Electron Laser Science, Hamburg, Germany. Since 2010, he has been a Researcher with the Institute for Photonics and Nanotechnology, National Research Council of Italy, Rome.

Paolo Farinello received the master's degree in engineering physics applied to nanooptics and photonics from Politecnico di Milano, Milan, Italy, in 2011. From 2011 to 2013, he joined the Department of Physics at Politecnico di Milano as a Research Fellow. Since then he started a Ph.D. program at the Laser Source Laboratory, University of Pavia, Pavia, Italy, working on solid-state lasers. His main research interest include the development and characterization of optical parametric amplifiers applied to time-resolved spectroscopy.

Giulio Cerullo is a Full Professor with the Physics Department, Politecnico di Milano, Milan, Italy. His research interests include ultrafast optical science and concerns the generation of few-optical-cycle tunable light pulses and their use to capture the dynamics of ultrafast events in molecular and solid-state systems.

Franz X. Kärtner heads the Ultrafast Optics and X-Rays Group with DESY CFEL, Hamburg, Germany, and is a Professor of physics with the University of Hamburg, Hamburg, and an Adjunct Professor of electrical engineering with the Massachusetts Institute of Technology, Cambridge, MA, USA. His research interests include noise in electronic and optical sources, ultrashort pulse lasers, high-energy sub-cycle waveform synthesis, and its use in precision timing in advanced accelerators and light sources, attosecond physics, and free-electron lasers.